Micro-Doppler Characteristics of Elderly Gait Patterns with Walking Aids

Moeness G. Amin[a], Fauzia Ahmad*[a], Yimin D. Zhang[a], and Boualem Boashash[b]

[a]Center for Advanced Communications, Villanova University, Villanova, PA 19085, USA
[b]Department of Electrical Engineering, College of Engineering, Qatar University, Doha, Qatar

ABSTRACT

In this paper, we analyze the micro-Doppler signatures of elderly gait patterns in the presence of walking aids using radars. The signatures are based on real data experiments conducted in a laboratory environment using human subjects walking with a walking cane and a walker. Short-time Fourier transform is used to provide the local signal behavior over frequency and to detail the changes in the micro-Doppler signatures over time. Intrinsic differences in the Doppler and micro-Doppler signatures of the elderly gait observed with and without the use of a walking aid are highlighted. Features that capture these differences can be effective in discriminating gait with walking aids from normal human gait.

Keywords: Micro-Doppler, human gait, assisted living, eldercare, walking aids.

1. INTRODUCTION

Independence-assisting technologies that can address the challenges of self-dependent living in homes and residences for the elderly population are an emerging area of research and development. The elderly population aged 65 years and above is growing and their ratio to the population aged 20-64 years in the United States is expected to reach 35% by 2030.[1] The worldwide population over 65 years is projected to increase to one billion by 2030. An overwhelming majority of these elderlies exercise self-care at their own homes most of the time or they are left unattended over short or extended periods of time in assisted living facilities. As such, personal emergency response systems are in high demand.

Radar based sensing has been brought to the forefront of indoor monitoring modalities in competition with cameras and wearable devices due to its attractive attributes related to its proven technology, privacy preservation, insensitivity to lighting conditions, and non-invasive nature.[2-7] Most of the personal emergency response systems focus on detection of falls, as these represent one of the leading causes of death in the elderly population.[8] Therefore, it is important for a sensing device to detect a fall irrespective of the preceding motion whether it is sitting, standing, or walking. Since many elderly use walking aids, such as canes or walkers, falls may progress from a gait that is different from a normal arm-leg swinging motion. Therefore, recognition of walking with a walking aid helps in characterizing the proper walk and detection of the transition from a walk to a fall.

In this paper, we consider the problem of human gait recognition in the presence of a walking aid using radars. We use time-frequency distributions to provide the local signal behavior over frequency and to detail the changes in the Doppler and micro-Doppler signatures over time.[9-15] We highlight the intrinsic differences in the time-frequency gait signatures with and without the use of a walking aid which, when captured by suitable features, can effectively discriminate the normal gait from that aided by a walking cane or a walker.

The remainder of the paper is organized as follows. In Section 2, we present the signal model. Section 3 reviews the short-time Fourier transform, which is commonly used for time-frequency analysis. The micro-Doppler signatures of elderly gait with and without walking aids, based on experimental data, are analyzed in Section 4, wherein the intrinsic differences between the considered signatures are demonstrated. Section 5 contains the concluding remarks.

*fauzia.ahmad@villanova.edu; http://www1.villanova.edu/villanova/engineering/research/centers/cac/facilities/rillab.html

2. SIGNAL MODEL

A monostatic continuous-wave (CW) radar transmits a sinusoidal signal, expressed as $s(t) = \exp(j2\pi f_c t)$, where f_c is the carrier frequency. Consider a point target which is located initially at a distance of R_0 from the radar, and moves with a velocity of $v(t)$ toward a direction that forms an angle θ with the radar line-of-sight. As such, the distance between the radar and the target at time instant *t* is

$$R(t) = R_0 + \int_0^t v(u)\cos(\theta)\, du, \tag{1}$$

and the received radar signal is expressed as

$$x_a(t) = \rho \exp\left[j2\pi f_c\left(t - \frac{2R(t)}{c}\right)\right], \tag{2}$$

where ρ *is* the target reflection coefficient and *c* is the velocity of the electromagnetic wave propagation. The Doppler frequency corresponding to $x_a(t)$ is

$$f_D(t) = 2v(t)\cos(\theta)/\lambda, \tag{3}$$

where $\lambda = c/f_c$ is the wavelength.

For a target with a spatial extent, such as a human body, the return signal is the integration over the target region **Ω**, expressed as

$$x(t) = \int_\Omega x_a(t)da. \tag{4}$$

In this case, the Doppler signature is the superposition of the component Doppler frequencies. Torso or gait motions generally generate time-varying Doppler frequencies, and their exact signatures depend on the target shape and motion patterns.

3. SHORT-TIME FOURIER TRANSFORM

By using joint time-frequency representations, the time-varying Doppler and micro-Doppler radar signatures can be captured with enhanced signal energy concentration at various time instants. Short-time Fourier transform (STFT) is a commonly used technique to perform time-frequency analysis.[16] The discrete-time STFT of signal $x(t)$ is defined as

$$X(t,f) = \sum_{m=-\infty}^{\infty} h(m)x(t-m)\exp(-j2\pi fm) \tag{5}$$

where t is the time index, f is the frequency, and $h(\cdot)$ is the discrete-time window function that trades off the time and frequency resolutions. A larger window length may degrade the time resolution whereas as a smaller window length may compromise the frequency resolution.

The spectrogram $S(t,f)$, which shows how the signal power varies with time index t and frequency f, is obtained by computing the squared magnitude of STFT of the signal $x(t)$,

$$S(t,f) = |X(t,f)|^2 = \left|\sum_{m=-\infty}^{\infty} h(m)x(t-m)\exp(-j2\pi fm)\right|^2. \tag{6}$$

In this paper, we use a Hamming window of length 255 for processing the data measurements.

4. ANALYSIS OF ELDERLY HUMAN GAIT WITH WALKING AIDS

4.1 Experimental Setup

A CW radar was set up in the Radar Imaging Lab at Villanova University. A vertically polarized horn antenna (BAE Systems, Model H-1479) with an operational frequency range of 1–12.4 GHz and 3-dB beamwidth of 45° was used as a transceiver for the monostatic radar. The feed point of the antenna was positioned 1.15 m above the floor. A network analyzer (Agilent ENA Series, Model E5071B) with an operational frequency range from 300 kHz to 8.5 GHz was used for signal generation and measurement of radar returns. A carrier frequency of 8 GHz was employed and the transmit power was set to 3 dBm. The network analyzer was externally triggered at a 1 kHz sampling rate. The radar return for each experiment was recorded for a duration of 20 seconds, resulting in a total of 20,000 data samples. The radar data were collected from different human subjects with direct line-of-sight to the targets. Both female and male subjects were asked to walk towards the radar, with and without a walking aid, between two points located at 4.5 m and 1 m from the antenna feed point, as shown in Fig. 1. An aluminum walking cane and an aluminum walker with wheels and a seat, both shown in Fig. 2, were chosen as the assistive devices. The specifications of the walking aids are provided in Table 1. The walker seat was raised up during data collection experiments. The experimental studies were approved by Villanova University's Institutional Review Board and were performed with consent from all participants.

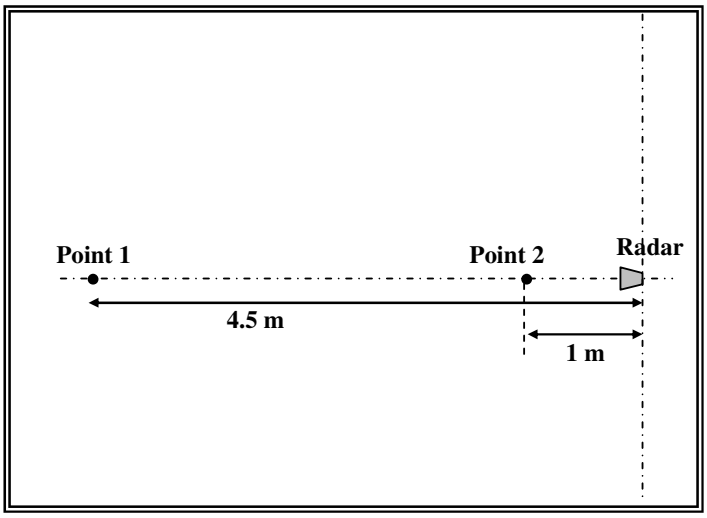

Figure 1. Scene layout.

4.2 Time-Frequency Analysis Results

We use spectrograms to capture the local signal behavior over frequency and changes in Doppler and micro-Doppler signatures over time for elderly gaits with and without walking aids. We first consider the elderly gait in the presence of a walking cane. Fig. 3 shows the spectrograms with a Hamming window of length 255, corresponding to two test subjects walking with the cane. In these and all subsequent figures, we plot the spectrograms on a 25 dB dynamic range. For comparison, Fig. 4 depicts the spectrograms corresponding to the same test subjects walking without any assistive device. In both Figs. 3 and 4, the strongest components correspond to the main motion of the torso, whereas the relatively weaker components capture the movements of the limbs (and cane in case of Fig. 3). Comparing Figs. 3 and 4, we observe the following two intrinsic differences. First, the radar return over one leg cycle is strengthened in the presence of the cane. This is because the motion of the cane is in sync with that of the leg, which causes an increase in intensity due to the combined scattering from the respective leg and the cane moving in concert. Second, owing to incremental time difference between the motion of the leg and that of the cane, the radar signature over one leg cycle is broader compared to that of the other leg cycle.

(a) (b)

Figure 2. Walking Aids, (a) Cane; (b) Walker.

Table 1. Specifications of the cane and walker.

WALKING CANE	WALKER
Material: Aluminum Length: 37 inches Diameter: 1 in	Material: Aluminum Height: 36 in Width: 22 in Depth: 20 in Seat: Plastic, 11 in deep

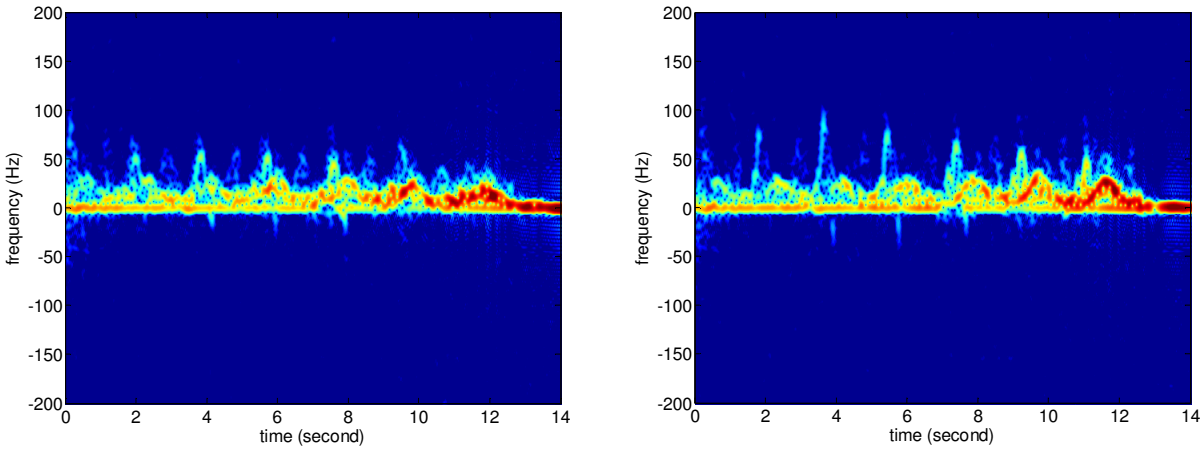

(b) (b)

Figure 3. Spectrogram of elderly gait with a walking cane, (a) Test subject 1; (b) Test subject 2. Strong return with lower positive Doppler is from the torso, whereas the weaker returns with high positive Doppler are from the legs and cane. The odd leg strides are stronger and broader than the even leg strides due to the presence of the cane.

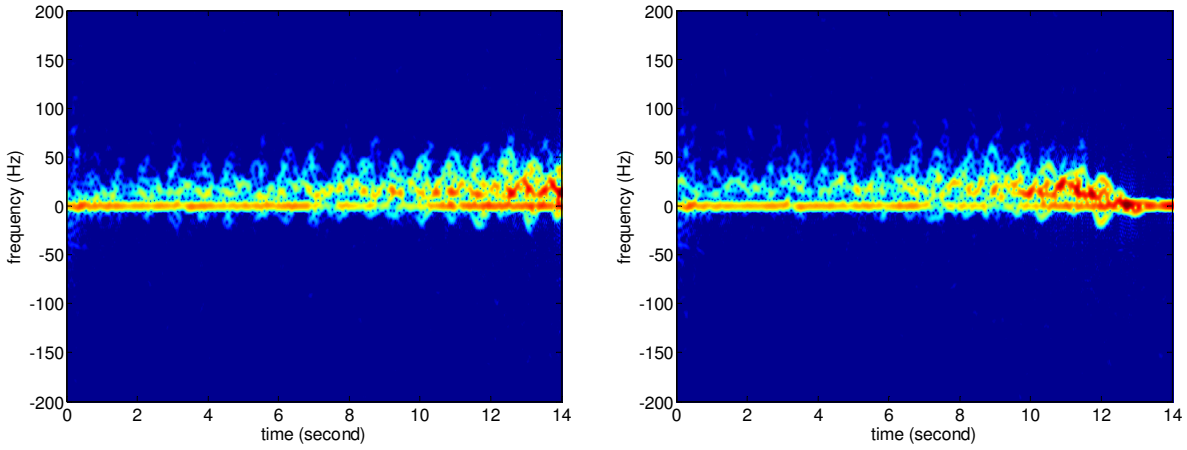

(c) (b)

Figure 4. Spectrogram of normal elderly gait, (a) Test subject 1; (b) Test subject 2. Strong return with lower positive Doppler is from the torso, whereas the weaker returns with positive and negative Doppler are from the limbs.

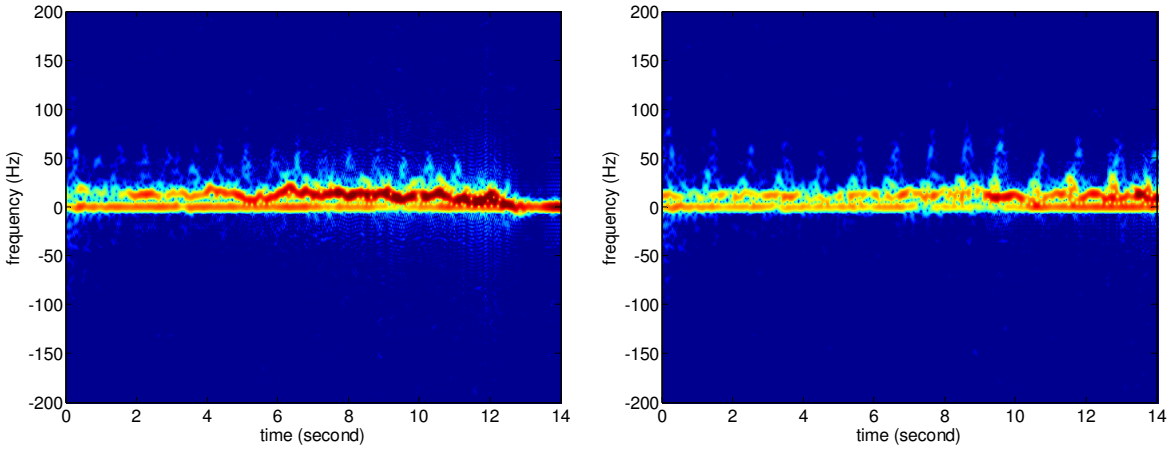

(a) (b)

Figure 5. Spectrogram of elderly gait with a walker, (a) Test subject 1; (b) Test subject 2. Strong return with lower positive Doppler is from the torso and the walker, whereas the weaker returns with the high positive Doppler are from the legs.

Next, we consider the elderly gait in the presence of a walker. Fig. 5 shows the spectrograms with a Hamming window of length 255, corresponding to the same two test subjects walking with the walker. We observe from Fig. 5 that the components capturing the movements of the limbs are relatively weak than those corresponding to the main motion of the torso and the walker. Comparing Figs. 4 and 5, we recognize the following intrinsic differences: 1) Negative Doppler when the object is moving towards the radar is almost non-existent due to lack of arm swinging in the opposite direction of motion, and 2) The radar return from the torso is strengthened in the presence of the walker. This is because the Doppler frequency shifts of the torso and the walker are similar and their combined effect causes an increase in intensity.

It is noted that features that effectively capture the aforementioned differences between the time-frequency signatures of the elderly gait, observed with and without the use of a cane and/or a walker, are expected to permit discrimination between the considered elderly gait patterns.

5. CONCLUSION

In this paper, we have demonstrated the differences in the radar signatures of the human gait observed with and without the use of a walking cane and a walker. Spectrograms were used to provide the time-varying Doppler and micro-Doppler signatures corresponding to the considered gaits. For the human gait with a walking cane, it was shown that the motion of the walking cane is in sync with that of the leg motion, leading to two main changes in the gait time-frequency signal representation, namely, strengthening of the radar return over one leg cycle and widening of the radar return over the same leg cycle. For the human gait with a walker, it was demonstrated that the torso and the walker signatures are merged together resulting in strengthening of the radar return from the torso compared to the case of walking with no walker. The recognition of the specific walking aid can help in characterizing the proper walk and detection of the transition from a walk to a fall.

ACKNOWLEDGMENT

This paper is made possible by Grant # NPRP 6-680-2-282 from the Qatar National Research Fund (a member of Qatar Foundation). The statements made herein are solely the responsibility of the authors.

REFERENCES

[1] AARP, "Health Innovation Frontiers: Untapped Market Opportunities for the 50+," (2013), <http://health50.org/files/2013/05/AARPHealthInnovationFullReportFINAL.pdf>

[2] Noury, N. et. al,"Fall detection - principles and methods," Proc. Annual Int. Conf. Engineering in Medicine and Biology Society, 1663–1666 (2007).

[3] Liu, L., Popescu, M., Skubic, M., Rantz, M., Yardibi, T., and Cuddihy, P., "Automatic fall detection based on Doppler radar motion signature," Proc. Int. Conf. Pervasive Computing Technologies for Healthcare and Workshops, Dublin, Ireland, (2011).

[4] Mercuri, M., Schreurs, D., and Leroux, P., "SFCW microwave radar for in-door fall detection," Proc. IEEE Topical Conf. Biomedical Wireless Technologies, Networks, and Sensing Systems, 53-56 (2012).

[5] Wu, M., Dai, X., Zhang, Y.D., Davidson, B., Zhang, J., and Amin M.G., "Fall detection based on sequential modeling of radar signal time-frequency features," Proc. IEEE Int. Conf. Healthcare Informatics, Philadelphia, PA, (2013).

[6] Gadde, A., Amin, M.G., Zhang, Y.D., and Ahmad, F., "Fall detection and classifications based on time-scale radar signal characteristics," Proc. SPIE 9077, Radar Sensor Technology XVIII, 907712 (2014).

[7] Wu, Q., Zhang, Y.D., Tao, W., and Amin, M.G., "Radar-based fall detection based on Doppler time-frequency signatures for assisted living," IET Radar, Sonar & Navigation, 9(2), 164-172 (2015).

[8] Englander F., Hodson T.J., and Terregrossa R.A., "Economic dimensions of slip and fall injuries," Journal of Forensic Science, 41(5), 733-746 (1996).

[9] Chen, V., [The Micro-Doppler Effect in Radar,], Artech House, Norwood, MA, (2011).

[10] Chen, V. and Ling, H., [Time-Frequency Transforms for Radar Imaging and Signal Analysis], Artech House, Norwood, MA, (2001).

[11] Amin, M.G., [Through-the-Wall Radar Imaging], CRC press, Boca Raton, FL, (2011).

[12] Clemente, C., Balleri, A., Woodbridge, K., and Soraghan, J., "Developments in target micro-doppler signatures analysis: radar imaging, ultrasound and through-the-wall radar," EURASIP Journal on Advances in Signal Processing, 2013:47 (2013).

[13] Amin, M., "Time-frequency spectrum analysis and estimation for nonstationary random-processes," in Time-Frequency Signal Analysis: Methods and Applications, B. Boashash, Longman Cheshire, (1992).

[14] Setlur, P., Ahmad, F., and Amin, M.G., "Analysis of micro-Doppler signals using linear FM basis decomposition," Proc. SPIE, Radar Sensor Technology X, 6210, 62100M (2006).

[15] Boashash, B., Khan, N.A., and Ben-Jabeur, T., "Time-frequency features for pattern recognition using high-resolution TFDs: A tutorial review," Digital Signal Process., 40, (2015).

[16] Almeida, L.B., "The fractional Fourier transform and time-frequency representations," IEEE Trans. Signal Proc., 42(11), 3084–3091 (1994).